

A combined experimental and DFT study of active structures and self-cycle mechanisms of mononuclear tungsten peroxy complexes in oxidation reactions

Peng Jin^a, Donghui Wei^a, Yiqiang Wen^a, Mengfei Luo^b, Xiangyu Wang^{a,*}, Mingsheng Tang^{a,*}

^a Department of Chemistry, Zhengzhou University, Zhengzhou, Henan 450052, China

^b Key Laboratory of the Ministry of Education for Advanced Catalysis Materials, Institute of Physical Chemistry, Zhejiang Normal University, Jinhua 321004, China

ARTICLE INFO

Article history:

Received 22 December 2010

Accepted 10 February 2011

Available online 15 February 2011

Keywords:

Active structure

Tungsten peroxy complex

Density functional theory (DFT)

Hydrogen peroxide

Adipic acid

ABSTRACT

Tungsten peroxy complexes have been widely used in olefin epoxidation, alcohol oxidation, Baeyer–Villiger oxidation and other oxidation reactions, however, there is still not a unanimous viewpoint for the active structure of mononuclear tungsten peroxy complex by now. In this paper, the catalysis of mononuclear tungsten peroxy complexes **0–5** with or without acidic ligands for the green oxidation of cyclohexene to adipic acid in the absence of organic solvent and phase-transfer catalyst has been researched in experiment. Then we have suggested two possible kinds of active structures of mononuclear tungsten peroxy complexes including peroxy ring (**nA**, $n = 0–1$) and hydroperoxy (**nB**, $n = 0–1$) structures, which have been investigated using density functional theory (DFT). Moreover, the calculations on self-cycle mechanisms involving the two types of active structures of tungsten peroxy complexes with and without oxalic acid ligand have also been carried out at the B3LYP/[LANL2DZ/6-31G(d, p)] level. The highest energy barrier are 26.17 kcal/mol (**0A**, peroxy ring structure without oxalic acid ligand), 23.91 kcal/mol (**1A**, peroxy ring structure with oxalic acid ligand), 18.19 kcal/mol (**0B**, hydroperoxy structure without oxalic acid ligand) and 13.10 kcal/mol (**1B**, hydroperoxy structure with oxalic acid ligand) in the four potential energy profiles, respectively. The results indicate that both the energy barriers of active structure self-cycle processes with oxalic acid ligands are lower than those without oxalic acid ligands, so the active structures with oxalic acid ligands should be easier to recycle, which is in good agreement with our experimental results. However, due to the higher energy of product than that of the reactant, the energy profile of the self-cycle process of **1B** shows that the recycle of **1B** could not occur at all in theory. Moreover, the crystal data of peroxy ring structure with oxalic acid ligand could be found in some experimental references. Thus, the viewpoint that the peroxy ring active structure should be the real active structure has been proved in this paper.

© 2011 Elsevier B.V. All rights reserved.

1. Introduction

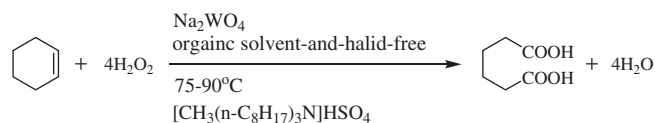
The peroxotungstates and peroxomolybdates have been widely used as high efficient catalysts for the oxidation of alcohols, sulfides and olefins [1–11], especially in the green oxidation reaction with hydrogen peroxide as oxidant. Hydrogen peroxide has high oxidation content and the only byproduct is water, so catalytic oxidations of organic substrates by H₂O₂ have been of growing interest [12–14]. Among these, the green syntheses of adipic acid with H₂O₂ as oxidant in the presence of tungsten species (tungsten peroxide species in particular) as catalysts are more attractive and have been successfully demonstrated.

Adipic acid is an important organic biacid which is used in the manufactures of nylon 6,6 and many other products [15]. It is

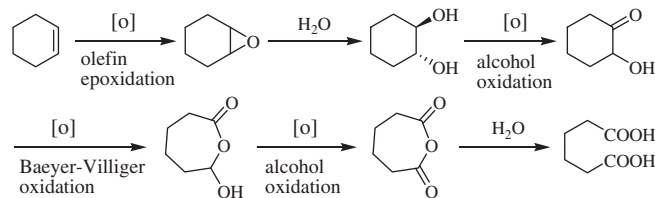
commonly prepared in industrial processes by oxidizing cyclohexanol or cyclohexanone using nitric acid. This reaction results in the formation of environmentally unfriendly nitrous oxide (N₂O) [16]. Thus, green routes to a direct synthesis of adipic acid are very desirable [17–24]. In recent years, the one-pot synthesis of adipic acid using H₂O₂ via homogeneous catalysis has been studied (Scheme 1), which can avoid the formation of N₂O [25]. According to the proposed pathway (Scheme 1), it should be stepwise mechanism in the reaction for the direct oxidation of cyclohexene to adipic acid with aqueous H₂O₂. From then on, many researchers have made a series of work continuously to promote the development of this method [30–34]. It has been well known that organic solvents using as improving agents, such as t-BuOOH, are usually introduced to increase reaction rates [26,27], and tungstates have received extensive attention for reactions of oxidative cleavage of alkenes in organic solvents [28,29]. However, organic solvents are also harmful to the environment and difficult to be disposed of. More recently, simple tungsten compounds [30–33] as catalysts

* Corresponding authors. Tel.: +86 371 67766076; fax: +86 371 67762210.

E-mail addresses: xiangyuwang@zzu.edu.cn (X. Wang), mstang@zzu.edu.cn (M. Tang).



The reported reaction of green synthesis of adipic acid



The proposed reaction pathway

Scheme 1. The reported reaction for the direct oxidation of cyclohexene to adipic acid with aqueous H₂O₂ and proposed pathway [25].

have been used to synthesize adipic acid with H₂O₂ as oxidant with the addition of quaternary ammonium compounds or acidic compounds as co-catalysts under organic solvents free conditions. Generally, acidic compounds are suggested as ligands with coordination effect on the stability and activity of tungsten compounds. In addition, Usui and Deng et al. [31,34] suggested that the oxidation actually occurred by the tungsten peroxide species, the tungsten-containing anion was converted to peroxotungstates in the course of the reaction. Thus, the tungsten peroxide species are essential to oxidation reactions.

To the best of our knowledge, there is still not a unanimous viewpoint for the active structure of mononuclear tungsten peroxo complex by now. On the one hand, Rösch et al. calculated that the tungsten peroxo complexes with bisperoxo groups instead of monoperoxo ones had higher activities for olefin epoxidation reaction using DFT/B3LYP method [35]. They thought W (O₂) three-membered ring formed the active group of catalyst. On the other hand, Mares et al. proposed that the W–O–O–H group would be the active group in alcohol oxidation reaction [1], which could efficiently transfer active oxygen like peracid and hydroperoxo (or alkylperoxo) groups, but this had not been proven by both of experiments and calculations. Which one is the real active structure of catalyst in these oxidation reactions?

In this work, our experimental study has been directed toward the exploring of catalysis of tungsten peroxo complexes (catalyst **0–5**, Table 1) for the green oxidation of cyclohexene to adipic acid. We found that, under the condition of only adding inorganic or organic acids as ligands with organic solvent and phase-transfer catalyst all free, the catalytic systems also have very excellent activities and the yields of adipic acid are high. Based on the experimental results and the reports [1,35], we are interested in studying what the real active structures of tungsten peroxo complexes used as catalysts are, so the two possible types of active structures for tungsten peroxo complexes involving **nA** and **nB** with oxalic acid ligand ($n = 1$, Scheme 2) and without oxalic acid ligand

Table 1
Yields of adipic acid in the presence of different tungsten peroxo complexes **0–5** as catalysts without organic solvent and phase-transfer catalyst.

Catalysts	Acidic ligand	Yield of adipic acid (wt.%)
0	–	81.0
1	Oxalic acid	92.0
2	Adipic acid	59.5
3	Phosphoric acid	86.7
4	Sulfuric acid	81.7
5	Hydrochloric acid	45.2

($n = 0$, Scheme 2) have been suggested and investigated by DFT theory in this article, which has been widely used in explaining many chemical problems [36–40]. Furthermore, in order to explain the activities and stabilities of these peroxo complexes, the self-cycle mechanisms of two active structures have also been investigated using the DFT theory.

2. Experimental and computational details

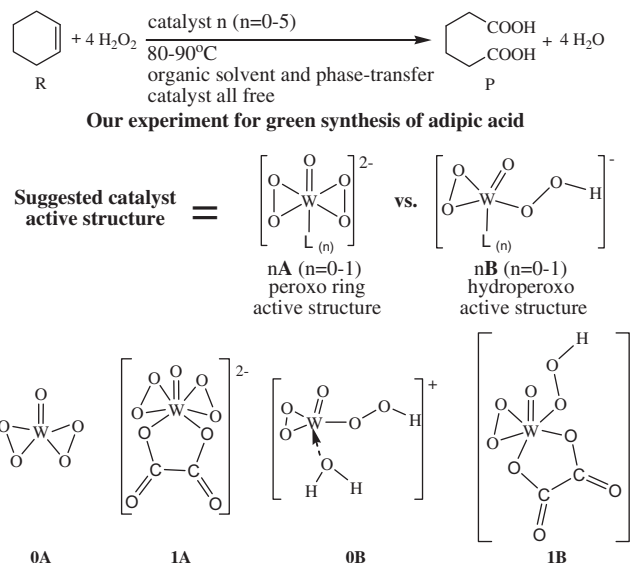
2.1. Reaction of green oxidation of cyclohexene to adipic acid

Reagents were purchased from Sinopharm Chemical Reagent Co., Ltd. Under the condition of organic solvent- and phase-transfer catalyst-free, the green synthesis of adipic acid via direct oxidation of cyclohexene by 30% H₂O₂ in the presence of tungsten peroxo complexes as catalysts have been investigated. Accurately measured the WO₃·H₂O, ligand (with or without) and H₂O₂ (30%) (the molar ratio is 1:1.1:220) were introduced in a 500 mL round-bottomed flask. The mixture was stirred 30 min for in situ preparation of catalyst and then cyclohexene (the molar ratio to H₂O₂ is 1:4.4) was added and the system was heated to keep reflux. After reflux, the system was stirred 6 h at 80–90 °C. When the reaction was over, the resulting hot solution was used for determination of the adipic acid yield by high performance liquid chromatography (HPLC).

HPLC analyses were carried out using Agilent 1100 HPLC system with a quaternary pump, an UV detector and a RID detector. HPLC separations were carried out on an Agilent TC-C18 reversed phase column (25 cm × 4.6 mm, 5 μm particle size) using a 30% methanol in 5 mM ammonium acetate buffer at pH 3.3 at 30 °C. UV data was collected at 225 nm.

2.2. Computational details

Density functional theory as implemented in the restricted B3LYP hybrid exchange correlation scheme was used to include some effects of electron correlation with only a marginal increase in computational cost over Hartree–Fock methods. All results have been obtained for cluster geometries optimized. W atom was modeled by a LANL2DZ effective core potential with additional



Scheme 2. The suggested two possible kinds of catalyst active structures participating in olefin epoxidation, alcohol oxidation, Baeyer–Villiger oxidation reactions and so on.

polarization (d-type) and diffuse (p-type) functions as developed by Check et al. [41]. A 6-31G(d, p) basis set was used for all other atoms.

All stationary points have been characterized with a full vibrational analysis, and all reported energy differences include zero point energy corrections. The corresponding vibrational frequencies were calculated at the same level to take account of the zero-point vibrational energy (ZPVE) and to identify the transition states. At the same time, the structures of intermediates and the transition states were confirmed by using the intrinsic reaction coordinate (IRC). All the theoretical calculations were performed using the Gaussian03 [42] suits of programs.

3. Results and discussion

3.1. Experimental results

In order to discover the activity of tungsten peroxo complexes, under the condition of organic solvent and phase-transfer catalyst all free, the green synthesis of adipic acid via direct oxidation of cyclohexene by 30% H₂O₂ with tungsten peroxo complexes with or without acidic ligand as catalysts **0–5** (Scheme 2) have been examined and the results are listed in Table 1.

As shown in Table 1, the kind of ligand in catalyst has a significant effect on the corresponding yield of adipic acid. From catalyst **1** to **5**, the corresponding yield of adipic acid reduces from 92.0 wt.% to 45.2 wt.%, and the trend is similar with the reported one [30].

3.2. The active structures of tungsten peroxo complexes

Considering the experimental results by the catalysts (catalyst *n*, *n* = 0–1) above, we are very interested in the role of oxalic acid ligand, and we want to compare the activities and stabilities of tungsten peroxo complexes with or without oxalic acid ligand (catalyst *n*, *n* = 0–1), moreover, we can not find any powerful experimental evidences to prove what the structure of complex **2**, **3**, **4**, **5** is. Thus, we will concentrate on oxalic acid complex and the complex without oxalic acid ligand only. Based on the reports [1,35], the two possible kinds of active structures for tungsten peroxo complexes (Scheme 2) have been suggested, which include peroxo ring (*nA*, *n* = 0–1) and hydroperoxo (*nB*, *n* = 0–1) active structures.

Many experimentally characterized bisperoxo complexes of tungsten that exhibited a pentagonal bipyramidal structure with a seven-coordinated metal center, the oxo and one ligand (or donor atom of a bidentate ligand) occupied axial positions, and the two peroxo groups and the remaining ligand were equatorial positions [43–45]. The calculated model complex **1A** (Fig. 1) that we have chosen also exhibits similar structure.

To analyze the model complex **1A**, we have compared the calculated geometry parameters to the results of X-ray analyses which is available for **1A** in Table 2.

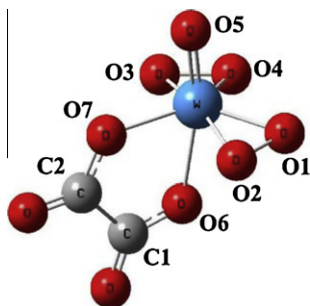


Fig. 1. Model complex **1A**.

As Table 2 displays, the calculated geometry of the model **1A** performs satisfactorily for the experimental structure of this complex. And **0A** is the same kind of tungsten peroxo complex with **1A**, while **nB** (*n* = 0–1) is formed by acidizing *nA* (*n* = 0–1). Hence, all the optimized geometric structures of *nA* and *nB* (*n* = 0–1) are obtained at the B3LYP/[LANL2DZ/6-31G(d, p)] level, which have been shown in Fig. 2. A vibrational frequency calculation was then performed at the optimized geometry belonging to each structure. We confirmed that *nA* and *nB* (*n* = 0–1) have no imaginary frequencies.

Some calculated important bond length of active structures of complex *nA* and *nB* are given in Table 3. As shown in Table 3, for each kind of active structure of tungsten peroxo complex (*nA* or *nB*, *n* = 0–1), the important structural parameters are similar.

3.3. The self-cycle mechanism of active structure

For interpreting the activities and stabilities of these peroxo complexes, the self-cycle mechanisms of two active structures have been calculated. Considering the suggested two active structures of tungsten peroxo complexes, the research result of peroxo ring active structure is firstly given in the following part.

3.3.1. The self-cycle mechanism of peroxo ring active structure

From experimental result above, we realize that oxalic acid ligand plays a very important role in the catalytic activity of tungsten peroxo complex. The self-cycle efficiency of catalyst not only influences the stability of its active structure, but also is closely related to the catalytic activity of catalyst. Thus, it is very necessary to research the role of oxalic acid ligand in self-cycle efficiency of active structure and to know the effect of structure on the performance of active structure. For these reasons, the self-cycle mechanisms of active structure involving with and without oxalic acid ligand have been investigated. We set the *E* + ZPVE of **M2** as 0.00 kcal/mol as reference in the energy profile of peroxo ring active structure without oxalic acid ligand, while we set the *E* + ZPVE of **M6** as 0.00 kcal/mol as reference in the energy profile of peroxo ring active structure with oxalic acid ligand (Fig. 4). The processes could be illustrated as follows:

3.3.1.1. The self-cycle mechanism of active structure without oxalic acid ligand (**0A**). The self-cycle mechanism of peroxo ring active structure without oxalic acid ligand (**0A**) has been suggested and the structures of intermediates and transition states are shown in Fig. 3.

There are two stages in this mechanism. First, it can be seen that after the peroxo ring group (O(1)–O(2)–W(3)) of **0A** participating in the catalytic oxidation reaction through a concerted oxygen-transfer step forms O(1)=W(3) in intermediate **M1**, the H₂O₂ will be close to **M1** to form **M2** via weak interaction in order to regenerate the peroxo ring active group. the O(4) atom of H₂O₂ attacks

Table 2
Comparison of calculated structures of **1A** with available experimental X-ray crystal data (distance unit: Å).

<i>r</i>	[WO(O ₂) ₂ (C ₂ O ₄) ²⁻] ₂ , calcd	[WO(O ₂) ₂ (C ₂ O ₄) ²⁻] ₂ , expt ^a
W–O(1)	1.94	1.93
W–O(2)	1.99	1.97
W–O(3)	1.99	1.97
W–O(4)	1.94	1.94
W–O(5)	1.73	1.72
W–O(6)	2.24	2.24
W–O(7)	2.07	2.14
O(1)–O(2)	1.48	1.51
O(3)–O(4)	1.48	1.50
C(1)–O(6)	1.29	1.29
C(2)–O(7)	1.32	1.29

^a Ref. [45].

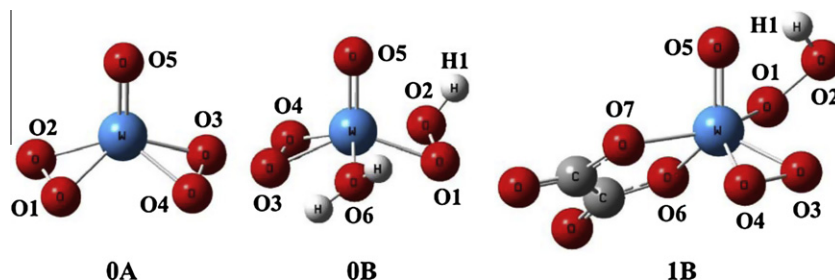


Fig. 2. The optimized active structures of complex nA and nB ($n = 0-1$, without $1A$).

Table 3

The calculated structures of nA and nB ($n = 0-1$, without $1A$, distance unit: Å).

r	0A	0B	1B
W–O(1)	1.92	1.95	1.98
W–O(2)	1.90	–	–
W–O(3)	1.90	1.90	1.92
W–O(4)	1.92	1.88	1.92
W–O(5)	1.70	1.69	1.72
W–O(6)	–	2.13	2.00
W–O(7)	–	–	2.05
O(1)–O(2)	1.47	1.47	1.45
O(3)–O(4)	1.47	1.46	1.48
H(1)–O(2)	–	0.99	0.98

the W(3) atom in $M2$ and the H(4) atom of H_2O_2 transfer to the O(1) atom of W(3)=O(1) bond to form $M3$ via a four-membered ring (W(3)–O(1)–H(4)–O(5)) transition state $TS1$. The energy barrier of this process is only 18.91 kcal/mol ($M2 \rightarrow TS1$, Fig. 4), which is not a high barrier. In addition, the distances of O(1)–W(3), H(4)–O(5), W(3)–O(5) and O(1)–H(4) change from 1.725 Å, 0.9760 Å, 2.172 Å and 2.923 Å in $M2$ to 1.803 Å, 1.243 Å, 2.104 Å and 1.259 Å in $TS1$, respectively. At last, the distances of W(3)–O(5) and O(1)–H(4) are 1.930 Å and 0.968 Å in $M3$, respectively. During the process of $M2$ converting to $M3$ via $TS1$, double-bond O(1)=W(3) become the single-bond while single-bond H(4)–O(5) disappear, and new single-bonds (W(3)–O(5), O(1)–H(4)) form. In other words, there are two bonds break so as to generate two new bonds.

Second, the O(6) atom of H_2O_2 attacks W(3) atom, and the H(7) atom of H_2O_2 is close to O(1) atom in $M3$ to generate $M4$ through transition state $TS2$. The energy barrier of this process is 26.17 kcal/mol ($M3 \rightarrow TS2$, Fig. 4), which is the highest energy barrier in the mechanism. In this process, two single-bonds

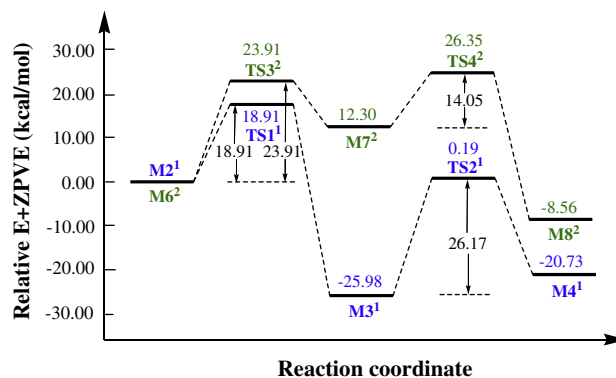


Fig. 4. The potential energy profiles of self-cycle mechanism of peroxy ring active structures at the B3LYP/[LANL2DZ/6-31G(d, p)] level (unit: kcal/mol, the superscript 1 represents active structures without oxalic acid ligand and the superscript 2 represents active structures with oxalic acid ligand).

(O(1)–W(3), O(6)–H(7)) break to generate two new bonds (W(3)–O(6), O(1)–H(7)). The distances of the O(1)–W(3), O(6)–H(7), W(3)–O(6) and O(1)–H(7) are 1.881 Å, 0.9760 Å, 2.459 Å and 3.847 Å in $M3$, and these distances change from 2.098 Å, 1.438 Å, 2.203 Å and 1.099 Å in $TS2$ to 2.196 Å, 2.487 Å, 1.922 Å and 0.9710 Å in $M4$, respectively. Attentively, O(5) and O(6) atoms in $M4$ are corresponding to O(2) and O(1) atoms in $0A$ (Fig. 3), respectively.

3.3.1.2. The self-cycle mechanism of active structure with oxalic acid ligand ($1A$). The self-cycle mechanism of this kind of complex with oxalic acid ligand ($1A$) is shown in Fig. 5, which is similar with that without oxalic acid ligand (Fig. 3).

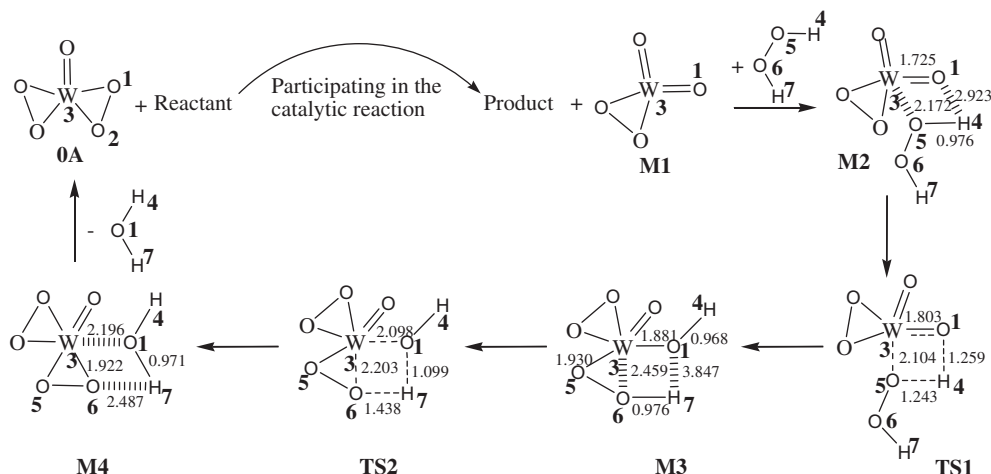


Fig. 3. The self-cycle mechanism of peroxy ring active structure without oxalic acid ligand (distance unit: Å, energy unit: kcal/mol).

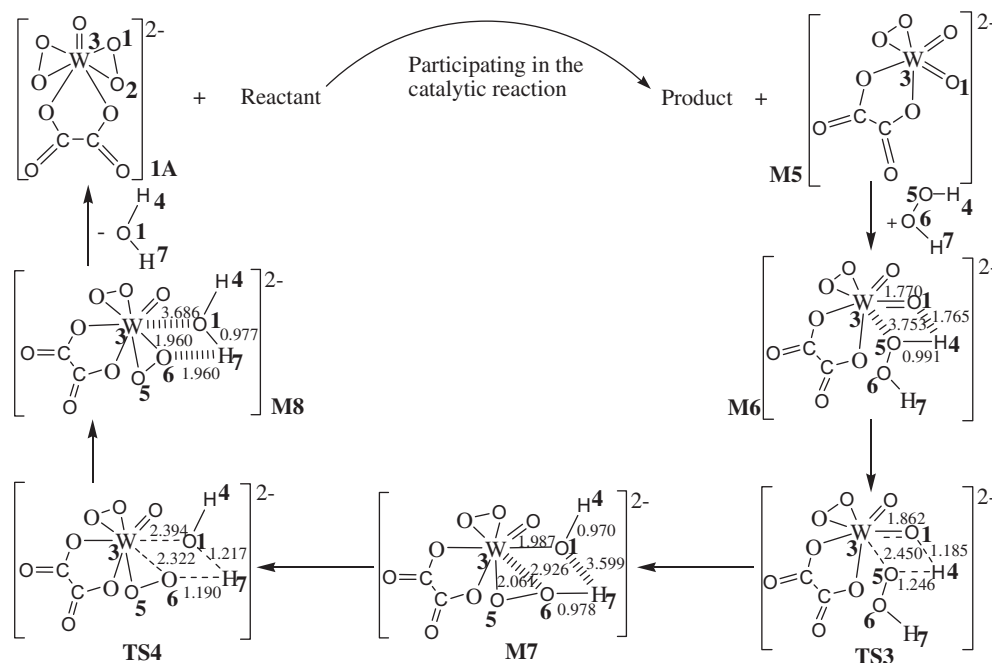


Fig. 5. The self-cycle mechanism of peroxy ring active structure with oxalic acid ligand (distance unit: Å, energy barrier unit: kcal/mol).

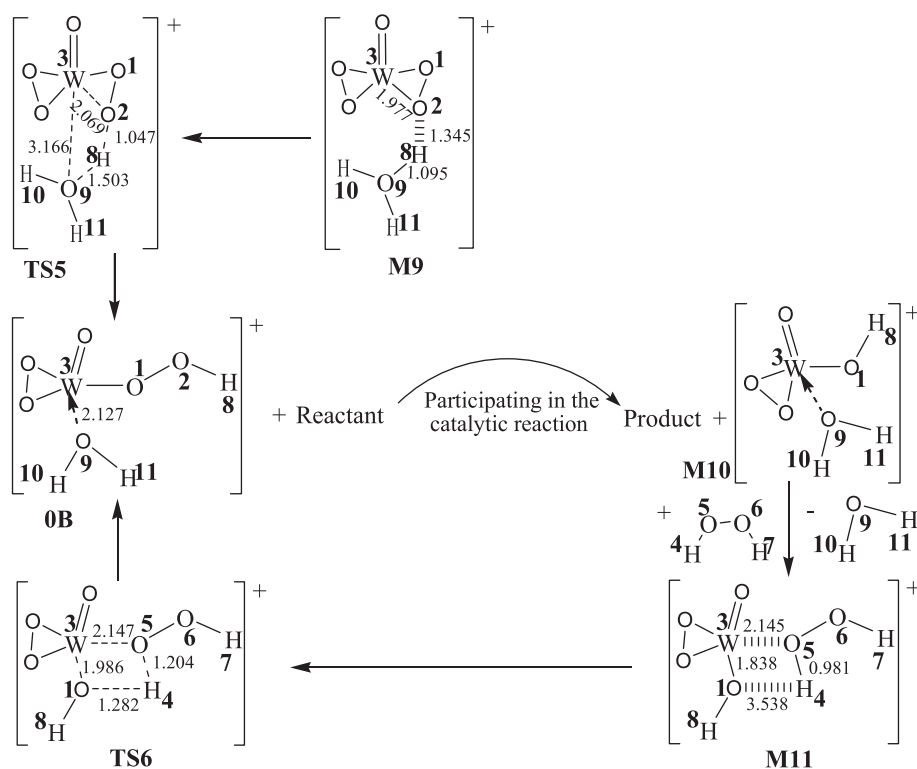


Fig. 6. The self-cycle mechanism of hydroperoxy active structure without oxalic acid ligand (distance unit: Å, energy barrier unit: kcal/mol).

The energy barrier of traversing the four-membered ring (W(3)–O(1)–H(4)–O(5)) transition state **TS3** is 23.91 kcal/mol (**M6** → **TS3**, Fig. 4). Moreover, the distances of O(1)–W(3), H(4)–O(5), W(3)–O(5) and O(1)–H(4) change from 1.770 Å, 0.9910 Å, 3.753 Å and 1.765 Å in **M6** to 1.862 Å, 1.246 Å, 2.450 Å and 1.185 Å in **TS3**, respectively. While the distances of W(3)–O(5) and O(1)–H(4) are 2.061 Å and 0.9700 Å in **M7**, respectively.

The energy barrier of the second step (traversing transition state **TS4**) is only 14.05 kcal/mol (**M7** → **TS4**, Fig. 4), which is 12.12 kcal/mol lower than that without oxalic acid ligand. The distances of the O(1)–W(3), O(6)–H(7), W(3)–O(6) and O(1)–H(7) are 1.987 Å, 0.9780 Å, 2.926 Å and 3.599 Å in **M7**, and these distances change from 2.394 Å, 1.190 Å, 2.322 Å and 1.217 Å in **TS4** to 3.686 Å, 1.960 Å, 1.960 Å and 0.9770 Å in **M8**, respectively.

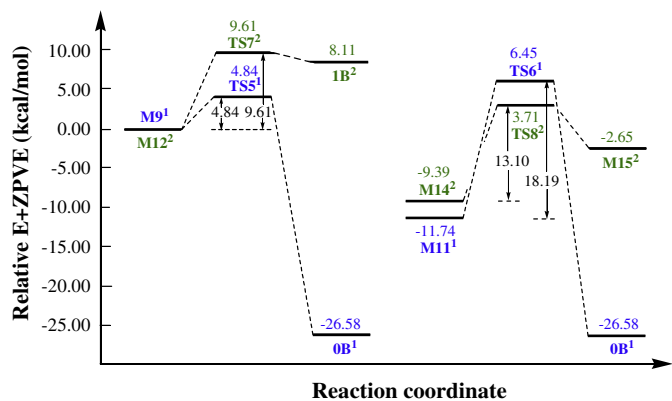


Fig. 7. The potential energy profiles of self-cycle mechanism of hydroperoxo active structures at the B3LYP/LANL2DZ/6-31G(d, p) level (unit: kcal/mol, the superscript 1 represents active structures without oxalic acid ligand and the superscript 2 represents active structures with oxalic acid ligand).

Noteworthy, O(5) and O(6) atoms in **M8** are corresponding to O(2) and O(1) atoms in **1A** (Fig. 5), respectively.

In addition, the highest energy barrier of cycle process of peroxy ring active structure without oxalic acid ligand is 26.17 kcal/mol (**M3** → **TS2**) in Fig. 4, while the highest energy barrier of cycle process of peroxy ring active structure with oxalic acid ligand is 23.91 kcal/mol (**M6** → **TS3**) in Fig. 4. It can be seen that the energy barrier of cycle process with oxalic acid ligand is 2.26 kcal/mol lower than that of cycle process without oxalic acid ligand, which shows that the cycle process of peroxy ring active structure with oxalic acid ligand is easier to proceed. And it is beneficial to recycle the active structure of complex as soon as possible in the catalytic reaction, which is very important not only for keeping active structure of complex stable, but also for promoting the catalytic reaction. Moreover, the computational trend of self-cycle processes (Fig. 4) is agreement with that of experiment (Table 1).

3.3.2. The self-cycle mechanism of hydroperoxo active structure

For the same reason with active structure **nA**, the self-cycle mechanisms of active structure **nB** containing with and without oxalic acid ligand have also been investigated. We set the *E* + ZPVE of **M9** as 0.00 kcal/mol as reference in the energy profile of hydroperoxo active structure without oxalic acid ligand, while we set the *E* + ZPVE of **M12** as 0.00 kcal/mol as reference in the energy profile of hydroperoxo active structure with oxalic acid ligand (Fig. 7).

3.3.2.1. The self-cycle mechanism of hydroperoxo active structure without oxalic acid ligand (**OB**). The structures of intermediates and transition states in the self-cycle mechanism of active structure **OB** have been depicted in Fig. 6, there are also two stages in this mechanism.

First, the protonhydrate in the solution system is close to **OA** (Scheme 2) to form intermediate **M9** and the H(8) atom of protonhydrate attacks the O(2) atom in **M9**, which generates **OB** through transition state **TS5**. The energy barrier of this process is only 4.84 kcal/mol (**M9** → **TS5**, Fig. 7), which is a very low barrier. In addition, the distances of O(2)–W(3), O(2)–H(8) and H(8)–O(9) change from 1.977 Å, 1.345 Å and 1.095 Å in **M9** to 2.069 Å, 1.047 Å and 1.503 Å in **TS5**, respectively, while the distance of W(3)–O(9) is 2.127 Å in **OB**. After the hydroperoxo (W(3)–O(1)–O(2)–H(8)) group of **OB** participating in the catalytic oxidation reaction with a concerted oxygen-transfer step to form W(3)–O(1)–H(8) in intermediate **M10**, the H₂O₂ will close to **M10** and the H₂O will go away to form **M11** via weak interaction.

Second, the O(5) atom of H₂O₂ attacks W(3) atom in **M11** and the H(4) atom of H₂O₂ is close to O(1) atom in **M11** to regenerate **OB** via transition state **TS6**. The energy barrier of this process is only 18.19 kcal/mol (**M11** → **TS6**, Fig. 7). During this process, two single-bonds (O(1)–W(3), H(4)–O(5)) break so as to generate two new bonds (W(3)–O(5), O(1)–H(4)). The distances of the O(1)–W(3), H(4)–O(5), W(3)–O(5) and O(1)–H(4) change from 1.838 Å, 0.981 Å, 2.145 Å and 3.538 Å in **M11** to 1.986 Å, 1.204 Å, 2.147 Å and 1.282 Å in **TS6**, respectively. Attentively, O(1), O(5),

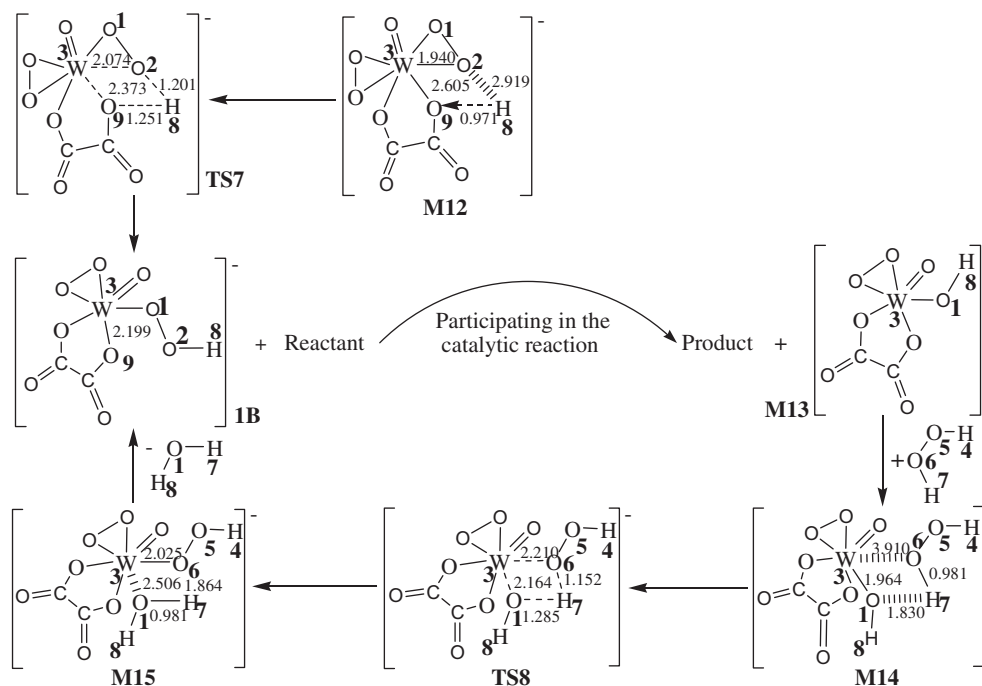


Fig. 8. The self-cycle mechanism of hydroperoxo active structure with oxalic acid ligand (distance unit: Å, energy barrier unit: kcal/mol).

O(6), H(4), H(7) and H(8) atoms in **TS6** are corresponding to O(9), O(1), O(2), H(11), H(8) and H(10) atoms in **OB** (Fig. 6), respectively.

3.3.2.2. The self-cycle mechanism of hydroperoxo active structure with oxalic acid ligand (1B). The self-cycle mechanism of hydroperoxo active structure with oxalic acid ligand (**1B**) is given in Fig. 8, which also has two stages as follows:

First, the dissociative H(8) atom which is derived from ligand is in the vicinity of anionic groups, when the system is heated, the H(8) atom will be close to **1A** (Scheme 2) to form bond (H(8)—O(9)) in intermediate **M12**. Then the H(8) atom attacks the O(2) atom in **M12** to generate **1B** via transition state **TS7**. The energy barrier of this process is only 9.61 kcal/mol (**M12** → **TS7**, Fig. 7). Moreover, the distances of O(2)—W(3), H(8)—O(9), W(3)—O(9) and O(2)—H(8) change from 1.940 Å, 0.971 Å, 2.605 Å and 2.919 Å in **M12** to 2.074 Å, 1.251 Å, 2.373 Å and 1.201 Å in **TS6**, respectively, while the distance of W(3)—O(9) is 2.199 Å in **1B**. In this process, two bond (O(2)—W(3), H(8)—O(9)) break so as to generate new bond (O(2)—H(8)). Then, the formed **1B** will participate in the catalytic reaction.

Second, the energy barrier of traversing the four-membered ring (W(3)—O(6)—H(7)—O(1)) transition state **TS8** is only 13.10 kcal/mol (**M14** → **TS8**, Fig. 7), which is 5.09 kcal/mol lower than that without oxalic acid ligand. The distances of the W(3)—O(6), O(1)—H(7), O(1)—W(3) and O(6)—H(7) are 3.910 Å, 1.830 Å, 1.964 Å and 0.981 Å in **M14** and these distances change from 2.210 Å, 1.285 Å, 2.164 Å and 1.152 Å in **TS8** to 2.025 Å, 0.9810 Å, 2.506 Å and 1.864 Å in **M15**, respectively. Noteworthy, O(6), O(5) and H(4) atoms in **M15** are corresponding to O(1), O(2) and H(8) atoms in **1B** (Fig. 8), respectively.

Compared the highest energy barrier of cycle process of **OB** (18.20 kcal/mol (**M11** → **TS6**) in Fig. 7) with that of **1B** (13.10 kcal/mol (**M14** → **TS8**) in Fig. 7), the energy barrier of cycle process with oxalic acid ligand is 5.10 kcal/mol lower than that without oxalic acid ligand, which also indicates that the self-cycle process of hydroperoxo active structure with oxalic acid ligand is more energy favorable. However, the reaction trend should be from right to left in the cycle process of **1B** (Fig. 7), which indicate that the self-cycle process of **1B** could not proceed. Thus, the hydroperoxo active structures may be unreasonable in theory.

4. Conclusion

In this paper, the exploring of catalysis of tungsten peroxo complexes for the green oxidation of cyclohexene to adipic acid in the absence of organic solvent and phase-transfer catalyst has been done in experiment, which indicates that the catalytic systems have very excellent activities. Based on the experimental results, the two possible types of active structures of tungsten peroxo complexes have been studied using the DFT/B3LYP method in theory, which include peroxo ring and hydroperoxo active structures. To interpret the activities and stabilities of these peroxo complexes in detail, the self-cycle mechanisms of two active structures have been investigated in this work. For both the active structures, self-cycle processes of active structures with oxalic acid ligand are more energy favorable than those without oxalic acid ligand, which demonstrates that the oxalic acid ligand plays a very significant role in promoting the catalytic reaction. As can be seen from the profiles of both the self-cycle processes (Figs. 4 and 7), although all the energy barriers in the profiles are not high at the experimental temperature and the B3LYP/6-31G(d, p) level, the energy of product is so higher than that of reactant in self-cycle process of **1B** that the reaction should be impossible to occur. Moreover, only the crystal data of peroxo ring structure with oxalic acid ligand could be found in the Refs. [43,45]. As concerned as

above, we think the peroxo ring active structure should be more reasonable. Furthermore, we will provide the further conclusion after we carefully research the complete mechanism of the green oxidation of cyclohexene to adipic acid in future.

Acknowledgments

We gratefully acknowledge the financial support from the innovation fund for Elitists of Henan province, China (Grants No. 0221001200).

Appendix A. Supplementary material

Supplementary data associated with this article can be found, in the online version, at doi:10.1016/j.molstruc.2011.02.023.

References

- [1] S.E. Jacobson, D.A. Muccigrosso, F. Mares, J. Org. Chem. 44 (1979) 921–924.
- [2] S. Sakaguchi, S. Watase, Y. Katayama, Y. Sakata, Y. Nishiyama, Y. Ishii, J. Org. Chem. 59 (1994) 5681–5686.
- [3] S. Sakaguchi, Y. Yamamoto, T. Sugimoto, H. Yamamoto, Y. Ishii, J. Org. Chem. 64 (1999) 5954–5957.
- [4] H. Yamamoto, M. Tsuda, S. Sakaguchi, Y. Ishii, J. Org. Chem. 62 (1997) 7174–7177.
- [5] W.S. Zhu, H.M. Li, X.Y. He, H.M. Shu, Y.S. Yan, J. Chem. Res. 12 (2006) 774–775.
- [6] W.P. Griffith, B.C. Parkin, A.J.P. White, D.J. Williams, J. Chem. Soc., Dalton Trans. (1995) 3131–3138.
- [7] X.Y. Shi, J.F. Wei, J. Mol. Catal. A: Chem. 229 (2005) 13–17.
- [8] K. Kamata, S. Kuzuya, K. Uehara, S. Yamaguchi, N. Mizuno, Inorg. Chem. 46 (2007) 3768–3774.
- [9] K. Kamata, T. Hirano, N. Mizuno, Chem. Commun. (2009) 3958–3960.
- [10] K. Kamata, T. Hirano, S. Kuzuya, N. Mizuno, J. Am. Chem. Soc. 131 (2009) 6997–7004.
- [11] K. Kamata, R. Ishimoto, T. Hirano, S. Kuzuya, K. Uehara, N. Mizuno, Inorg. Chem. 49 (2010) 2471–2478.
- [12] V. Nardello, J.M. Aubry, D.E. De Vos, R. Neumann, W. Adam, R. Zhang, J.E. ten Elshof, P.T. Witte, P.L. Alsters, J. Mol. Catal. A: Chem. 251 (2006) 185–193.
- [13] J. Hofmann, U. Freier, M. Wecks, A. Demund, Top. Catal. 33 (2005) 243–247.
- [14] G. Grigoropoulou, J.H. Clark, J.A. Elings, Green Chem. 5 (2003) 1–7.
- [15] A. Castellán, J.C.J. Bart, S. Cavallaro, Catal. Today 9 (1991) 237–254.
- [16] M.H. Thiemens, W.C. Troglor, Science 251 (1991) 932–934.
- [17] R. Noyori, M. Aoki, K. Sato, Chem. Commun. (2003) 1977–1986.
- [18] M. Dugal, G. Sankar, R. Raja, J.M. Thomas, Angew. Chem. Int. Ed. 39 (2000) 2310–2313.
- [19] R. Raja, G. Sankar, J.M. Thomas, Angew. Chem. Int. Ed. 39 (2000) 2313–2316.
- [20] A. Chavan, D. Srinivas, P. Ratnasamy, J. Catal. 212 (2002) 39–45.
- [21] G.P. Scindler, P. Bartl, W.F. Hoelderich, Appl. Catal. A: Gen. 166 (1998) 267–279.
- [22] R. Raja, S.O. Lee, M.S. Sanchez, G. Sankar, K.D.M. Harris, B.F.G. Johnson, J.M. Thomas, Top. Catal. 20 (2002) 85–88.
- [23] R. Raja, J.M. Thomas, M.C. Xu, K.D.M. Harris, H.M. Greenhill, K. Quill, Chem. Commun. (2006) 448–450.
- [24] G. Lapisardi, F. Chiker, F. Launay, J.P. Nogier, J.L. Bonardet, Catal. Commun. (2004) 277–281.
- [25] K. Sato, M. Aoki, R.A. Noyori, Science 281 (1998) 1646–1647.
- [26] T. Oguchi, T. Ura, Y. Ishii, M. Ogawa, Chem. Lett. 18 (1989) 857–860.
- [27] Y. Ishii, K. Yamawaki, T. Ura, H. Yamada, T. Yoshida, M. Ogawa, J. Org. Chem. 53 (1988) 3587–3593.
- [28] C. Venturello, E. Alneri, M. Ricci, J. Org. Chem. 48 (1983) 3831–3833.
- [29] C. Venturello, M. Ricci, Eur. Pat. Appl. EP 122804 (1984).
- [30] H. Jiang, H. Gong, Z. Yang, X.T. Zhang, Z.L. Sun, React. Kinet. Catal. Lett. 75 (2002) 315–321.
- [31] Y. Usui, K. Sato, Green Chem. 5 (2003) 373–375.
- [32] W.S. Zhu, H.M. Li, X.Y. He, Q. Zhang, H.M. Shu, Y.S. Yan, Catal. Commun. 9 (2008) 551–555.
- [33] P.U. Maheswari, X.H. Tang, R. Hageb, P. Gameza, J. Reedijk, J. Mol. Catal. A: Chem. 258 (2006) 295–301.
- [34] Y.Q. Deng, Z.F. Ma, K. Wang, J. Chen, Green Chem. 1 (1999) 275–276.
- [35] C. Di Valentin, P. Gisdakis, I.V. Yudanov, N. Rösch, J. Org. Chem. 65 (2000) 2996–3004.
- [36] A.I. Francisco, M.D. Vargas, J.W. de, M. Carneiro, M. Lanzaster, J.C. Torres, C.A. Camara, A.C. Pinto, J. Mol. Struct. 891 (2008) 228–232.
- [37] Z. Džolić, M. Cetina, D. Kovaček, A. Hergold-Brundić, D. Mrvoš-Sermeek, A. Nagl, N. Slade, K. Pavelić, J. Balzarini, E.D. Clercq, O. Zerbe, G. Folkers, L. Scapozza, M. Mintas, J. Mol. Struct. 655 (2003) 229–241.
- [38] (a) D.H. Wei, M.S. Tang, J. Zhao, L. Sun, W.J. Zhang, C.F. Zhao, S.R. Zhang, H.M. Wang, Tetrahedron: Asymmetry 20 (2009) 1020–1026; (b) D.H. Wei, M.S. Tang, J. Phys. Chem. A 113 (2009) 11035–11041;

- (c) D.H. Wei, W.J. Zhang, Y.Y. Zhu, M.S. Tang, *J. Mol. Catal. A Chem.* 326 (2010) 41–47.
- [39] G. Huerta, L. Fomina, *J. Mol. Struct. (THEOCHEM)* 761 (2006) 107–112.
- [40] S. Olsztynska-Janus, K. Szyborska, M. Komorowska, J. Lipinski, *J. Mol. Struct. (THEOCHEM)* 911 (2009) 1–7.
- [41] C.E. Check, T.O. Faust, J.M. Bailey, B.J. Wright, T.M. Gilbert, L.S. Sunderlin, *J. Phys. Chem. A* 105 (2001) 8111–8116.
- [42] M.J. Frisch, G.W. Trucks, H.B. Schlegel, G.E. Scuseria, M.A. Robb, J.R. Cheeseman, J.A. Montgomery Jr., T. Vreven, K.N. Kudin, J.C. Burant, J.M. Millam, S.S. Iyengar, J. Tomasi, V. Barone, B. Mennucci, M. Cossi, G. Scalmani, N. Rega, G.A. Petersson, H. Nakatsuji, M. Hada, M. Ehara, K. Toyota, R. Fukuda, J. Hasegawa, M. Ishida, T. Nakajima, Y. Honda, O. Kitao, H. Nakai, M. Klene, X. Li, J.E. Knox, H.P. Hratchian, J.B. Cross, C. Adamo, J. Jaramillo, R. Gomperts, R.E. Stratmann, O. Yazyev, A.J. Austin, R. Cammi, C. Pomelli, J.W. Ochterski, P.Y. Ayala, K. Morokuma, G.A. Voth, P. Salvador, J.J. Dannenberg, V.G. Zakrzewski, S. Dapprich, A.D. Daniels, M.C. Strain, O. Farkas, D.K. Malick, A.D. Rabuck, K. Raghavachari, J.B. Foresman, J.V. Ortiz, Q. Cui, A.G. Baboul, S. Clifford, J. Cioslowski, B.B. Stefanov, G. Liu, A. Liashenko, P. Piskorz, I. Komaromi, R.L. Martin, D.J. Fox, T. Keith, M.A. Al-Laham, C.Y. Peng, A. Nanayakkara, M. Challacombe, P.M.W. Gill, B. Johnson, W. Chen, M.W. Wong, C. Gonzalez, J.A. Pople, *Gaussian 03, Revision C. 02*, Gaussian, Inc., Wallingford CT, 2004.
- [43] R. Stomberg, S. Olson, *Acta Chem. Scand., Ser. A* A39 (1985) 79–83.
- [44] M.H. Dickman, M.T. Pope, *Chem. Rev.* 94 (1994) 569–584.
- [45] X.B. Shi, C.G. Li, S.H. Wu, J. Chen, G.Y. Xie, *Chin. Sci. Bull.* 39 (1994) 1886–1889.